20th International Conference on Information Fusion
Xi'an, China - July 10-13, 2017

Robust track-to-track association algorithm based on t-distribution mixture model

Baozhu Li, Ningbo Liu, Guoqing Wang, Lin Qi, Yunlong Dong
Institute of Information Fusion
Naval Aeronautical and Astronautical University, Yantai, China
E-mail:libaozhu1324@163.com

***Abstract*—To address multi-sensor robust track-to-track association in the presence of sensor biases and missed detections, where sensors biases is time-varying and non-uniform, the target of different sensors is non-identical, the robust track-to-track association algorithm based on t-distribution mixture model is proposed. The robust track-to-track association problem is turned into the non-rigid point matching problem. Firstly, the orthogonal normalization reduce the general affine case of track point set; second, the heavy-tailed t-distribution mixture model is established with better robustness to tracks of non-common, solved by Expectation Maximization (EM) algorithm. The conditional expectation function is added a regular item of point sets that the points have a feature of Coherent Point Drift (CPD). Adaptability experiments are established to demonstrate the effectiveness of the proposed approaches compared with competing algorithms at the presence of sensor biases and missed detections.**

Keywords—Track association; Sensor biases; t-distribution mixture model; Expectation Maximization algorithm; Coherent Point Drift

I. INTRODUCTION

It is widely recognized that track-to-track association is a crucial technique in the distributed multi-sensor fusion system, which distinguishing tracks of the same targets from different sensors, eliminating redundant tracks, merging the same tracks, and achieving better surveillance performance in the complex environment [1,2]. When the sensors have different surveillance regions and missed detections, the target sets detected by local sensors isn't coincide, which will be difficult to determine correspondence between local tracks from different sensors. In addition, in the presence of sensor bias, estimated states deviate greatly from the true states. In this case, it becomes more difficult to perform track-to-track association.

To solve the above problems of track-to-track association under sensor biases, a large number of literatures have studied. In [3], the Fourier transform is used to estimate the rotation and translation between tracks and compensate. In [4], a method using maximum likelihood rule to estimate the sensor biases and applying the K-best algorithm to perform track-to-track association. In the literature [5], the similarity of the topology is imposed on the algorithm by using the method of constant distance between targets. However, the robustness of the association algorithm decreases with the larger of the sensor biases. The literature [6] constructs a novel mixed integer nonlinear programming model in the maximum likelihood rule, which assuming that the sensor biases are imposed on the original sensor measurements. In [7], the OSPA distance is imposed, and the robust track-to-track association based on the reference topology feature has been proposed. For the case of missed detections, the literature [8] imposed the target estimation state and its covariance, which is globally optimized on the basis of deriving the statistical distance of the topology, and adopts the double threshold criterion. However the algorithm needs to traverse the search calculation, the algorithm is not efficient. The literature [9] constructs pseudo-measurement model which imposing the Taylor series expansion to register sensor biases and track-to-track association. But, the method can only deal with the small sensor biases, Convergence speed is slow, and the calculation is complicated [10]. In [11], a method based on distance detection is proposed according to the statistical characteristics of Gaussian random vectors, which derives a distance vector between homologous tracks, rough association based on minimum average and refines association based on χ^2 distribution. Zhu turned the Robust track-to-track association algorithm problem into the non-rigid point set matching problem in [12] [13]. In [12], a relaxation labeling is imposed on the algorithm. The framework of TPS-RPM2 is applied in [13].

In this paper, we mainly address the problem of robust track-to-track association in the presence of sensor biases and non-common observation. A robust track-to-track association based on the t-distribution mixture models is proposed, which inspired by the non-rigid point set matching. The rest of the paper is organized as follows. The problem from the view of the point set matching is formulated in Section II. Section III depicts flow of algorithm, including orthogonal normalization, t-distribution mixture models establishment and solution. Simulation and the performance of the algorithm are given in Section IV, followed by conclusions in Section V.

This work was supported in part by the National Natural Science Foundation of China(61401495,61471382,61501487, 61531020), The Natural Science Foundation of Shandong Province (2015ZRA06052)

978-0-9964-5270-0©2017 ISIF

II. Problem Formulation

Consider a multi-target tracking scenario with two sensors and several targets in the distributed surveillance region. The Global Cartesian Coordinate System is established with location of sensor 1 as the coordinate origin, and (x_{2s}, 0) is the location of sensor 2. In references with the radar which measures the range and azimuth to the target, the measurement process is implemented in the Local Polar Coordinate System. Let (r_m^i, θ_m^i) as the *i*th measurement from sensor *m* (m=1, 2) at time instant *k*. Due to the presence of sensor bias and random measurement errors,

$$\begin{bmatrix} r_m^i \\ \theta_m^i \end{bmatrix} = \begin{bmatrix} \overline{r}_m^i \\ \overline{\theta}_m^i \end{bmatrix} + \begin{bmatrix} \Delta r_m \\ \Delta\theta_m \end{bmatrix} + \begin{bmatrix} v_{m,r} \\ v_{m,\theta} \end{bmatrix} \tag{1}$$

Where $\overline{r}_m^i$ denotes the real range of the *i*th target to the sensor *m*, $\overline{\theta}_m^i$ denotes the real azimuth of the *i*th target to the sensor *m*; Δr_m denotes sensor bias on range, $\Delta\theta_{\mathrm{m}}$ denotes sensor bias on azimuth; $v_{\mathrm{m},r}$ and $v_{\mathrm{m},\theta}$ denote range random error and azimuth random error, respectively. Assuming that estimated state of the *i*th target is $(\hat{\mathrm{x}}_m^i, \hat{\mathrm{y}}_m^i)$ in the Global Cartesian Coordinate System, and the real location is $(\overline{\mathrm{x}}, \overline{\mathrm{y}})$, the random error in the measurement process is ignored. At the sensor m

$$\begin{aligned} \hat{x}_m^i &= (\overline{r}_m^i + \Delta r_m)\cos(\overline{\theta}_m^i + \Delta\theta_m) \\ \hat{y}_m^i &= (\overline{r}_m^i + \Delta r_m)\sin(\overline{\theta}_m^i + \Delta\theta_m) \end{aligned} \tag{2}$$

Let $\theta_0 = \Delta\theta_1 - \Delta\theta_2$, if the two tracks are from the same target (*i*=*j*), we have

$$\begin{aligned} \begin{bmatrix} \hat{x}_2^j \\ \hat{y}_2^j \end{bmatrix} &= \frac{\overline{r}_2^j + \Delta r_2}{\overline{r}_2^j} \frac{\overline{r}_1^i}{\overline{r}_1^i + \Delta r_1} \begin{bmatrix} \cos\theta_0 & \sin\theta_0 \\ -\sin\theta_0 & \cos\theta_0 \end{bmatrix} \begin{bmatrix} \hat{x}_1^i \\ \hat{y}_1^i \end{bmatrix} \\ &- \frac{\overline{r}_2^j + \Delta r_2}{\overline{r}_2^j} \begin{bmatrix} (\frac{\overline{r}_2^j + 2\Delta r_2}{\overline{r}_2^j + \Delta r_2} - \cos\Delta\theta_2) x_{2s} \\ x_{2s}\sin\Delta\theta_2 \end{bmatrix} \end{aligned} \tag{3}$$

from (2).

When Δr_1 and Δr_2 are very small and ignored. At this point, we rewrite the (3) as

$$\begin{bmatrix} \hat{x}_2^i \\ \hat{y}_2^j \end{bmatrix} = \begin{bmatrix} \cos\theta_0 & \sin\theta_0 \\ -\sin\theta_0 & \cos\theta_0 \end{bmatrix} \begin{bmatrix} \hat{x}_1^i \\ \hat{y}_1^j \end{bmatrix} - \begin{bmatrix} (1-\cos\Delta\theta_2) x_{2s} \\ x_{2s}\sin\theta_2 \end{bmatrix} \tag{4}$$

It can be seen from (4), with the azimuth biases only or small range biases, two local estimated state from the same target can be mapped by the rotation and translation transformation. However, with the range random error of the sensor is large (as in (3)); it is a non-rigid transformation between two local estimated states.

III. Track-to-Track Association Based on the T-Distribution Mixture Model

Since the rigid transformation is a special case of non-rigid transformation, the local tracks from different sensors, which originating from the same target, can be described by non-rigid transformations. Therefore, this paper transforms the problem of track association into the non-rigid point set matching problem by t-distribution mixed models establishment, solved by EM algorithm with considering the Coherent Point Drift of the track point.

In Global Cartesian Coordinate System, given two point sets $\boldsymbol{X} = \{\boldsymbol{X}_i\}_{i=1}^N$ and $\boldsymbol{Y} = \{\boldsymbol{Y}_j\}_{j=1}^M$ constituted by biased local tracks of sensor 1 and sensor 2, the purpose of track-to-track association is to determine the correspondence between two point sets. Where $\boldsymbol{X}_i$ and $\boldsymbol{Y}_j$ denote the D-dimensional estimated state of the *i*th and *j*th target, respectively. N and M denote the number of target tracked by the sensors 1 and 2, respectively.

A. Orthogonal Normalization of Tracks Point Set

The objective orthogonal normalization is to simplify the general affine transformation problem as a rotation only rigid body transformation problem [14]. Orthogonal normalization is divided into the following three steps:

- Eliminate the effect of translation parameters

$$\begin{aligned} \boldsymbol{X}' &= \boldsymbol{X} - \mathbf{1}_{N\times 1}\cdot m(\boldsymbol{X}) \\ \boldsymbol{Y}' &= \boldsymbol{Y} - \mathbf{1}_{M\times 1}\cdot m(\boldsymbol{Y}) \end{aligned} \tag{5}$$

where *m*(.) denotes the mean value of point sets, $\boldsymbol{1}_{M*1}$ denotesthe column vector with all elements of 1.

- Seek the simple matrix of orthogonal normalization

$$\begin{aligned} \boldsymbol{S}_{X'} &= (\boldsymbol{X}')^T \cdot \boldsymbol{X}' \\ \boldsymbol{S}_{Y'} &= (\boldsymbol{Y}')^T \cdot \boldsymbol{Y}' \end{aligned} \tag{6}$$

where $\mathrm{S_X}$ and $\mathrm{S_Y}$ denote the second order matrix of $\boldsymbol{X}'$ and $\boldsymbol{Y}'$, respectively.

- Calculate the orthogonal normalization of the original point set:

$$\begin{aligned} \tilde{\boldsymbol{X}} &= (\boldsymbol{S}_{X'}^{-1/2})^T \cdot \boldsymbol{X}' \\ \tilde{\boldsymbol{Y}} &= (\boldsymbol{S}_{Y'}^{-1/2})^T \cdot \boldsymbol{Y}' \end{aligned} \tag{7}$$

After the original point set has been subjected to orthogonal normalization transformation, there is only a rotation transformation relationship between the obtained orthogonal normalization point sets.

B. t-distribution Mixture Model Formulation

Assuming that the track point set $\tilde{\boldsymbol{X}}$ is regarded as the set of sample points in the point set registration, the track set $\tilde{\boldsymbol{Y}}$ is the set of floating points. $\tilde{\boldsymbol{Y}}_j$ is the centroid of the Gaussian distribution mixture models (GMM) [15,16], the GMM probability density function (p.d.f)for $\tilde{\boldsymbol{X}}_i$

$$f(\tilde{\boldsymbol{X}}_i; \tilde{\boldsymbol{Y}}_j, \omega_j, \sigma^2 I) = \sum_{j=1}^{M} \omega_j f_N(\tilde{\boldsymbol{X}}_i; \tilde{\boldsymbol{Y}}_j, \sigma^2 I) \tag{8}$$

$$f_N(\tilde{\boldsymbol{X}}_i; \tilde{\boldsymbol{Y}}_j, \sigma^2 I) = \frac{1}{\left(2\pi\sigma^2\right)^{D/2}} \exp\left(-\frac{\left\|\tilde{\boldsymbol{X}}_i - \tilde{\boldsymbol{Y}}_j\right\|^2}{2\sigma^2}\right) \tag{9}$$

where the ω_j denotes the a priori weight of $\tilde{\boldsymbol{Y}}_j$ in the mixed density function, $\sigma^2 I$ denotes the covariance matrix.

We use a component normal mixture p.d.f for the targets being detected by sensor 1, and not by sensor 2. Introducing a weight of this distribution as ε to the mixture model, we get

$$f_N(\tilde{\boldsymbol{X}}_i;\tilde{\boldsymbol{Y}}_j,\sigma^2 I) = (1-\varepsilon) f_N(\tilde{\boldsymbol{X}}_i;\tilde{\boldsymbol{Y}}_j,\sigma^2 I) + \varepsilon f_N(\tilde{\boldsymbol{X}}_i;\tilde{\boldsymbol{Y}}_j,c\sigma^2 I) \qquad (9)$$

where c is large and ε is small, representing the small proportion of observations that have a relatively large variance.

The normal scale mixture model (9) can be written as

$$f(\tilde{\boldsymbol{X}}_i;\tilde{\boldsymbol{Y}}_j,\sigma^2 I) = \int f_N(\tilde{\boldsymbol{X}}_i;\tilde{\boldsymbol{Y}}_j,\sigma^2 I/u)dH(u) \qquad (10)$$

Where H is the probability distribution that places mass $(1-\varepsilon)$ at the point $u=1$ and mass ε at the point $u=1/c$. Suppose $H(u)$ is χ^2 random with degrees of freedom γ; that is, by the random variable U distributed as

$$U \sim \text{gamma}(\gamma/2,\gamma/2) \qquad (11)$$

From (10), we can obtain t distribution with variable $\tilde{\boldsymbol{X}}_i$

$$f(\tilde{\boldsymbol{X}}_i;\tilde{\boldsymbol{Y}}_j,\omega_j,\boldsymbol{\Sigma},\gamma_j) = \sum_{j=1}^{M}\omega_j f_T(\tilde{\boldsymbol{X}}_i;\tilde{\boldsymbol{Y}}_j,\boldsymbol{\Sigma},\gamma_j) \qquad (12)$$

$$f_T(\tilde{\boldsymbol{X}}_i;\tilde{\boldsymbol{Y}}_j,\boldsymbol{\Sigma},\gamma_j) = \frac{\Gamma(\frac{\gamma_j+D}{2})}{|\Sigma|^{1/2}\left[\gamma_j\Gamma(\frac{1}{2})\right]^{D/2}\Gamma(\frac{\gamma_j}{2})\left[1+d(\tilde{\boldsymbol{X}}_i,\tilde{\boldsymbol{Y}}_j,\boldsymbol{\Sigma})\right]^{\frac{\gamma_j+D}{2}}} \qquad (13)$$

where, Γ(·) denotes the Gamma function, γ_j denotes the degree of freedom of the t-distribution function, $d(\tilde{\boldsymbol{X}}_i,\tilde{\boldsymbol{Y}}_j,\boldsymbol{\Sigma})$ represents the Mahalanobis distance between $\tilde{\boldsymbol{X}}_i$ and $\tilde{\boldsymbol{Y}}_j$.

C. Solved t-distribution Mixture Models by EM Algorithm

In general, the optimal solution of the t-distribution mixed model parameters ω, σ, γ is difficult to obtain, and the gradient descending flow is usually used. In this paper, we apply the EM algorithm to estimate the parameters. The EM algorithm needs to introduce a complete set of data. Therefore, we define a complete set of data$\boldsymbol{\Psi}$=($\tilde{\boldsymbol{X}}$;z_1,…,z_N;u_1,…,u_N), where z_i=(z_{i1},…,z_{iM}), u denotes the implicit data set in the EM algorithm. When z_{ij}=1, it indicates that the target *i* is associated with the target *j*; otherwise, z_{ij} = 0. For the z and u

$$u_i\Big|_{z_{ij}=1} \sim f_\Gamma(\frac{1}{2}\gamma_j,\frac{1}{2}\gamma_j)$$
$$\tilde{\boldsymbol{X}}_i\Big|_{u_i,z_{ij}=1} \sim f_N(\tilde{\boldsymbol{Y}}_j,\sigma^2/u_i) \qquad (14)$$

We define the parameter set $\boldsymbol{\Phi}$=(ω,σ,γ). Substituting (13) and (14) into (12), we can get the logarithmic likelihood function of the t-distribution mixture models of the point set $\tilde{X}$

$$\ln(\tilde{\boldsymbol{X}},\tilde{\boldsymbol{Y}}|\boldsymbol{\Phi}) = \ln L_1(\omega_j) + \ln L_2(\gamma_j) + \ln L_3(\boldsymbol{Y}_j,\sigma^2) \qquad (15)$$

where,

$$\ln L_1(\omega_j) = -\sum_{i=1}^{N}\sum_{j=1}^{M} z_{ij}\ln\omega_j$$
$$\ln L_2(\gamma_j) = -\sum_{i=1}^{N}\sum_{j=1}^{M} z_{ij}[-\ln\Gamma(\frac{\gamma_j}{2}) + \frac{1}{2}\gamma_j\ln(\frac{\gamma_j}{2}) + \frac{1}{2}\gamma_j(\ln u_j - u_j) - \ln u_j]$$
$$\ln L_3(\boldsymbol{Y}_j,\sigma^2) = -\sum_{i=1}^{N}\sum_{j=1}^{M} z_{ij}\left[-\frac{D\ln(2\pi)}{2} - \ln\sigma^2 - \frac{u_j\left\|\tilde{\boldsymbol{X}}_i-\tilde{\boldsymbol{Y}}_j\right\|^2}{2\sigma^2}\right] \qquad (16)$$

The essence of the EM algorithm [17] is to seek the expectation of (15) and use the iterative method to solve the parameter set $\boldsymbol{\Phi}$. EM algorithm is divided into E-step and M-step two iterative process:

- E-step

We need to minimize the condition expectation of the parameter set $\boldsymbol{\Phi}$, when performing the (*k*+1)th iteration calculation E-step to get parameter set $\boldsymbol{\Phi}$.

$$Q(\boldsymbol{\Phi};\hat{\boldsymbol{\Phi}}^{(k)}) =$$
$$\mathrm{E}_{X_B|X_A,\hat{\Phi}_n}\ln(\tilde{\boldsymbol{X}},\tilde{\boldsymbol{Y}}|\boldsymbol{\Phi}) = -\sum_{i=1}^{N}\sum_{j=1}^{M} p(\tilde{\boldsymbol{Y}}_j^{(k)};\tilde{\boldsymbol{X}}_i)\ln\left[\omega_j f(\tilde{\boldsymbol{X}}_i;\tilde{\boldsymbol{Y}}_j^{(k)},(\sigma^2)^{(k)},\gamma_j^{(k)})\right] \qquad (17)$$

Where, $p(\tilde{\boldsymbol{Y}}_j^{(k)};\tilde{\boldsymbol{X}}_i)$ denotes the posterior probability density of the t-distributed mixed component

$$p(\tilde{\boldsymbol{Y}}_j^{(k+1)};\tilde{\boldsymbol{X}}_i) = p_{ij}^{(k+1)} = \frac{\omega_j^{(k)} f_t(\tilde{\boldsymbol{X}}_i;\tilde{\boldsymbol{Y}}_j^{(k)},(\sigma^2)^{(k)},\gamma_j^{(k)})}{\sum_{j=1}^{M}\omega_j^{(k)} f_t(\tilde{\boldsymbol{X}}_i;\tilde{\boldsymbol{Y}}_j^{(k)},(\sigma^2)^{(k)},\gamma_j^{(k)})} \qquad (18\ )$$

In addition, since $p_{\Phi^{(k+1)}}(u_j;\tilde{\boldsymbol{X}}_i,\mathrm{z}_{ij}=1)$ and $p_{\Phi^{(k+1)}}(\ln u_j;\tilde{\boldsymbol{X}}_i,\mathrm{z}_{ij}=1)$ are included in the derivation of (18), we also need calculate

$$u_{ij} = p_{\Phi^{(k+1)}}(u_j;\tilde{\boldsymbol{X}}_i,\mathrm{z}_{ji}=1) = \frac{\gamma_j^{(k)}+D}{\gamma_j^{(k)}+d(\tilde{\boldsymbol{X}}_i,\tilde{\boldsymbol{Y}}_j,(\sigma^2)^{(k)})} \qquad (\ 19)$$

$$p_{\Phi^{(k+1)}}(\ln u_j;\tilde{\boldsymbol{X}}_i,\mathrm{z}_{ji}=1) = \ln u_{ij}^{(k+1)} + \psi(\frac{\gamma_j^{(k)}+D}{2}) - \ln\frac{\gamma_j^{(k)}+D}{2} \qquad (20\ )$$

Where $\psi(\cdot)$ denotes the Digamma function.

- M-step

Substituting (18), (19) and (20) into (17), we rewrite the original system as follows:

$$Q(\boldsymbol{\Phi};\hat{\boldsymbol{\Phi}}^{(k)}) = Q(\omega_j;\hat{\boldsymbol{\Phi}}^{(k)}) + Q(\gamma_j;\hat{\boldsymbol{\Phi}}^{(k)}) + Q(x_j,\sigma^2;\hat{\boldsymbol{\Phi}}^{(k)}) \qquad (\ 21)$$

$$Q(\omega_j^{(k+1)};\hat{\boldsymbol{\Phi}}^{(k)}) = -\sum_{i=1}^{N}\sum_{j=1}^{M} p_{ij}^{(k+1)}\ln\omega_j^{(k)} \qquad (22\ )$$

$$Q(\gamma_j^{(k+1)};\hat{\boldsymbol{\Phi}}^{(k)}) = -\sum_{i=1}^{N}\sum_{j=1}^{M} p_{ij}^{(k+1)} \left\{ -\ln\Gamma(\frac{\gamma_j^{(k)}}{2}) + \frac{\gamma_j^{(k)}}{2}\ln\frac{\gamma_j^{(k)}}{2} \right.$$
$$\left. + \frac{\gamma_j^{(k)}}{2}\left[\sum_{i=1}^{N}(\ln u_{ij}^{(k)} - u_{ij}^{(k)}) + \psi(\frac{\gamma_j^{(k)}+D}{2})\right] - \ln\frac{\gamma_j^{(k)}+D}{2} \right\} \tag{23}$$

$$Q(\tilde{\boldsymbol{Y}}_j^{(k+1)},(\sigma^2)^{(k+1)};\hat{\boldsymbol{\Phi}}^{(k)}) = -\sum_{i=1}^{N}\sum_{j=1}^{M} p_{ij}^{(k+1)} \left[-\frac{D\ln(2\pi)}{2} \right.$$
$$\left. -\frac{\ln(\sigma^{2D})^{(k)}}{2} + \frac{D\ln u_{ij}^{(k)}}{2} + \frac{u_{ij}^{(k)}\left\|\tilde{\boldsymbol{X}}_i - \tilde{\boldsymbol{Y}}_j\right\|^2}{2(\sigma^2)^{(k)}} \right] \tag{24}$$

where (24) denotes a desired value function containing the estimated states $\tilde{X}$ and $\tilde{\boldsymbol{Y}}$.

When (22) is maximized, we can obtain

$$\omega_j^{(k+1)} = \underset{\Phi}{\arg\max}\ Q(\omega_j^{(k+1)};\hat{\Phi}^{(k)}) = \frac{1}{N}\sum_{i=1}^{N} p_{ij}^{(k+1)} \tag{25}$$

When (23) is maximized, $\gamma_j^{(k+1)}$ is the solution of

$$-\psi(\frac{\gamma_j^{(k+1)}}{2}) + \ln\frac{\gamma_j^{(k+1)}}{2} + 1 + \frac{1}{\sum_{i=1}^{N} p_{ij}^{(\mathrm{k})}}\cdot\left[\sum_{i=1}^{N}(\ln u_{ij}^{(k)} - u_{ij}^{(k)})\right]$$
$$+\psi(\frac{\gamma_j^{(k)}}{2}) + \ln\frac{\gamma_j^{(k)}+D}{2} = 0 \tag{26}$$

In order to solve $\gamma_j^{(k+1)}$, we impose ECM algorithm [18] for iteration solution. In the solution of (24), the correspondence relation of the associated track is unknown and non-exclusive. In order to ensure the consistency of motion between track points and avoid the wrong association of many to one, Tikhonov regular term [19] is imposed in the paper as penalty function in (24).

D. Tikhonov Regularization

We define the displacement vector of the point set $\tilde{\boldsymbol{Y}}$ as $T(\tilde{Y},\nu) = \tilde{Y} + \nu(\tilde{Y})$. Then, the regular term $\varphi(v)$ is added to the $Q(\tilde{\boldsymbol{Y}}_j^{(k+1)},(\sigma^2)^{(k+1)};\hat{\Phi}^{(k)})$, we rewrite (24) as follow

$$\hat{Q}(\nu) = Q(\tilde{\boldsymbol{Y}}_j,\sigma^2;\boldsymbol{\Phi}) + \frac{\lambda}{2}\phi(\nu) \tag{27}$$

where λ denotes the weight coefficient of the Tikhonov regular term, and the larger the λ is, the better the regularity, and the more accurate the match. According to the literature [17], we can get

$$T(\tilde{Y},\nu) = \tilde{Y} + \nu(\tilde{Y}) = \tilde{Y} + GR \tag{28}$$

where G denotes an M×M-dimensional Gaussian kernel matrix: $g_{mn} = \exp\left(-\left\|\tilde{\boldsymbol{Y}}_m - \tilde{\boldsymbol{Y}}_n\right\|^2 / 2\beta^2\right)$.

Substituting (24), (28) into (27),

$$\hat{Q}(\nu) = -\sum_{i=1}^{N}\sum_{j=1}^{M} p_{ij}^{(k+1)} \left[-\frac{D\ln(2\pi)}{2} - \frac{\ln(\sigma^{2D})^{(k)}}{2} + \frac{D\ln u_{ij}^{(k)}}{2} \right.$$
$$\left. + \frac{u_{ij}^{(k)}\left\|\tilde{\boldsymbol{X}}_i - \tilde{\boldsymbol{Y}}_j^{(k)} - \boldsymbol{G}_{j,\cdot}\boldsymbol{R}\right\|^2}{2(\sigma^2)^{(k)}} \right] + \frac{\lambda}{2}\mathrm{tr}\left(\boldsymbol{R}^{\mathrm{T}}\boldsymbol{G}\boldsymbol{R}\right) \tag{29}$$

where $\boldsymbol{G}_{j,\cdot}$ denotes the row vector of the Gaussian kernel matrix. In the regular theory, the Gaussian kernel matrix G has the effect of low-pass filtering to enhance the motion consistency between the track points; β is the smoothness coefficient, and β>0, the bigger the β, the smoother the matching result; the weight matrix of G dimension.

Since (29) is a function of ***R*** and σ^2, minimized and solved

$$\boldsymbol{R} = \left[\mathrm{diag}(\boldsymbol{P1})\boldsymbol{G} + \lambda\sigma^2\boldsymbol{I}\right]^{-1}\left[\hat{\boldsymbol{P}}\tilde{\boldsymbol{X}} - \mathrm{diag}(\hat{\boldsymbol{P}}\boldsymbol{1})\tilde{\boldsymbol{Y}}\right] \tag{30}$$

where P_{ij} denotes matrix elements of **P**, **1** is the column vector of element 1, and ***I*** is the unit matrix.

The solution of $\partial\hat{Q}(v)/\partial\sigma^2 = 0$

$$(\sigma^2)^{(k+1)} = \frac{\sum_{i=1}^{N}\sum_{j=1}^{M} p_{ij}^{(k+1)} u_{ij}^{(k+1)} \left\|\tilde{\boldsymbol{X}}_i - \tilde{\boldsymbol{Y}}_j^{(k+1)} - \boldsymbol{G}_{j,\cdot}\boldsymbol{R}\right\|^2}{D\sum_{i=1}^{N}\sum_{j=1}^{M} p_{ij}^{(k+1)} u_{ij}^{(k+1)}} \tag{31}$$

IV. SIMULATION AND ANALYSIS

A. Simulation Environment

To evaluate the performance of the proposed algorithm, we consider a multiple target tracking scenario with two sensors. Sensor 1 is located at (0km,0km), and sensor 2 is located at (150km,0km).There are 20 targets distributed uniformly in the region [65km,120km]×[65km,120km]. The range random errors for both sensors are modeled as white Gaussian noises with standard deviations $\sigma_r^1 = 60$ m and $\sigma_r^2 = 80$ m. The azimuth random errors are also modeled as white Gaussian noises with standard deviations $\sigma_\theta^1 = 0.4°$ and $\sigma_\theta^2 = 0.3°$. Both the value and the direction of initial velocity obeys uniform distribution, v_0~U(5m/s,200m/s), θ_0~U(0, 2π rad). The simple interval t is 1 s, and the running time is 300s. The range biases of the two sensors areΔr_1=200m and Δr_2=200m, and the azimuth biases of the two sensors are $\Delta\theta_1$ =1°and $\Delta\theta_2$=-1°. The detection probabilities of the two sensors are P_{D1}=0.9 and P_{D2}=0.7. 50 Monte-Carlo simulation runs are conducted for the experiment results.

Performance comparisons are made between the proposed algorithm and the competing algorithms, including FFT algorithm and TPS-RPM2. The association performance is evaluated by the average probability of correct association

$$P_C = \frac{1}{MK}\sum_{i=1}^{M}\sum_{t=1}^{T}\frac{N_C^i(t)}{N'(t)} \tag{32}$$

where, N' denotes the total number of common targets, N_C^i denotes the correctly associated targets number at the ith Monte-Carlo run. M denotes the number of Monte-Carlo run, K denotes running time.

B. Simulation results and analysis

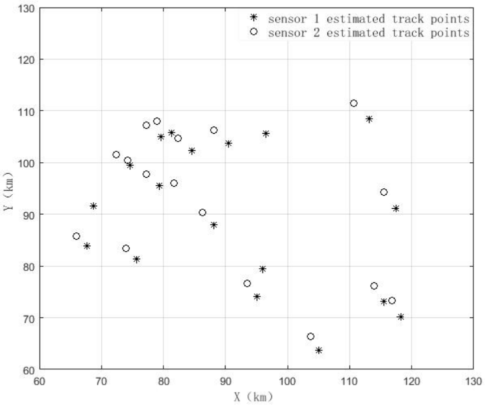

Fig. 1. Track points of sensors before association

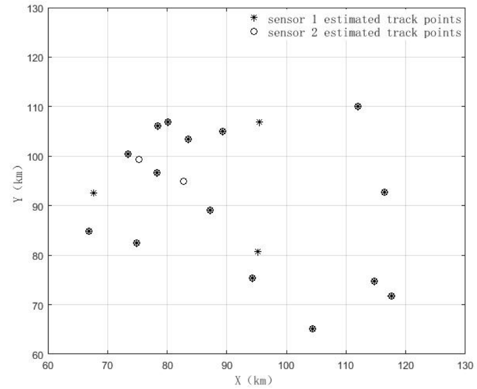

Fig. 2. Track points of sensors after association

Fig.1 depicts the original multi-target locations given by different sensors when the detection probabilities of the two sensors are P_{D1}=0.9 and P_{D2}=0.7. Fig.2 illustrates the effectiveness of track points after association by the proposed algorithm. It can be seen that when the sensor observation targets are not exactly the same, the proposed algorithm can effectively carry out the association of the track points.

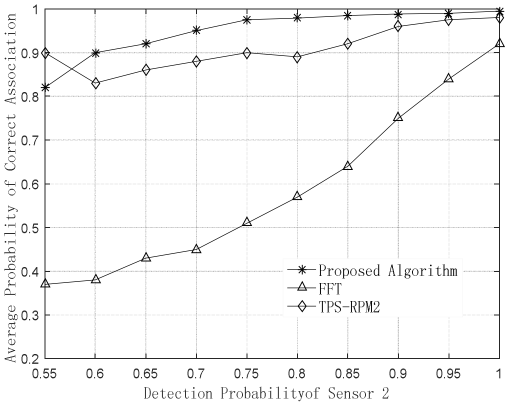

Fig. 3. Average probability of correct association via different detection probability

Figs.3–6 illustrate the average probabilities of correct association via different detection probabilities, range biases, azimuth biases and the total numbers of targets, respectively. In fig.3, the detection probability P_{D1} of sensor 1 is 0.9, and the detection probability P_{D2} of sensor 2 varies from 0.55 to 1. Form fig.3, it is shown that the proposed algorithm outperform the other competing algorithms. As the detection probability increase, the probabilities of correct association of the proposed approaches present a steady rise. With small detection probability, the correct association probability of algorithm proposed is better than FFT algorithm and TPS-RPM2. It because that t-distribution mixture models have better robustness to anomaly point and noise, with the increase of the detection probability, the correct association probability of this algorithm can rise close to 1 more quickly.

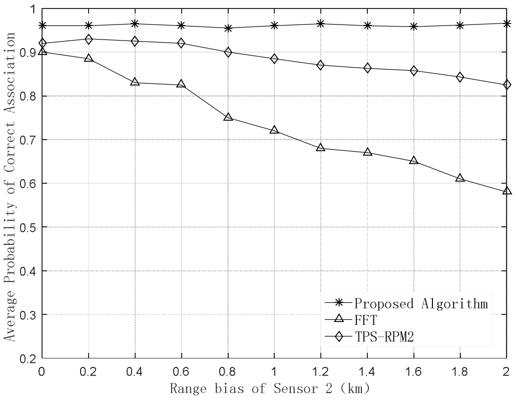

Fig. 4. Average probability of correct association via different range bias

In fig.4, the range bias Δr_1 of sensor 1 is 200m, and the range bias Δr_2 of sensor 2 varies from 0 to 2km. Fig.4 indicates that, with small range bias, all the 3 methods share high correct association rates. However, as the rising of sensor range biases, the performance of FFT algorithm and TPS-RPM2 experience degradation to some extent. Whereas, the performance of the proposed algorithm is relatively stable, and the robustness to the range bias is better.

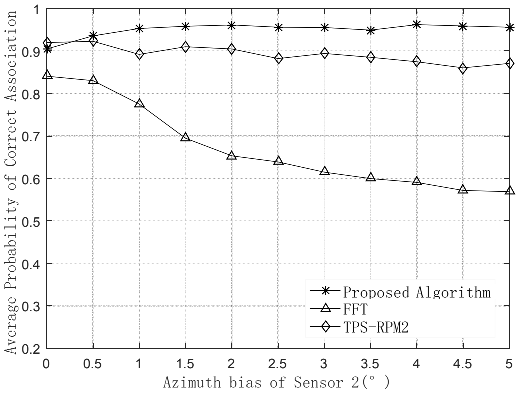

Fig. 5. Average probability of correct association in different azimuth bias

In fig.5, the azimuth biases $\Delta\theta_1$ of sensor 1 is =1°, and the azimuth biases$\Delta\theta_2$ of sensor 2 varies from 0 to 5°. It is seen that from fig.5, as the azimuth biases increase, the performance of FFT and TPS-RPM2 degraded. However, the proposed algorithm is not sensitive to the azimuth bias, with better robustness for azimuth bias.

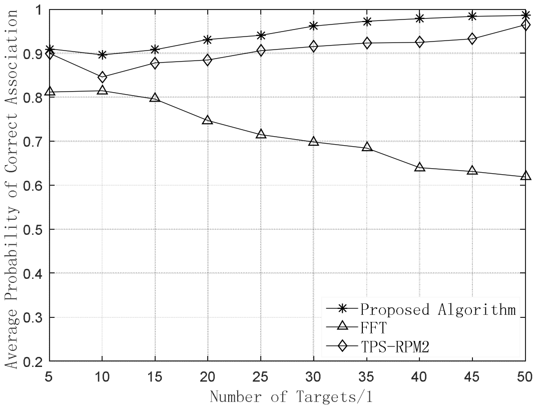

Fig. 6. Average probability of correct association via the total number of targets

In Fig. 6, the total number of targets varies from 5 to 50, both of range bias Δr_1 and Δr_2 are 200m, the azimuth biases $\Delta\theta_1$ and$\Delta\theta_2$ are 1° and -1°, respectively. As shown in fig.6, with the small number of targets, all the three algorithms are good track association performance. As the total number of targets increases, correct data association of FFT is hindered by the strong interference from a large number of targets. However, the proposed approaches and TPS-RPM2 still produce good association results, and the performance of the proposed algorithm is better.

TABLE I. AVERAGE RUNNING TIME OF ALGORITHM

total number of targets	**Average Running Time of Algorithm** (seconds)		
	FFT	***TPS-RPM2***	***Proposed Algorithm***
10	***0.3725***	***0.5143***	***0.4731***
20	***0.3738***	***1.6378***	***1.3152***
30	***0.3753***	***2.4360***	***2.1056***
40	***0.3769***	***3.9125***	***3.6739***
50	***0.4108***	***5.2013***	***4.9251***

Table I illustrate the average single running time of the algorithms based on the following computer configuration: CPU: Intel (R) Core (TM) i5 CPU 760 @ 2.80 GHz; RAM: 8 GB; Operating system: Windows 7. As shown in Table I, as the total number of targets increases, the time required for each algorithm has increased. The proposed approaches and TPS-RPM2 are more time-consuming. Although the FFT is time-efficient, it fails to produce good results for the track-to-track association.

V. Conclusions

This paper proposes a new algorithm to the problem of robust track-to-track association in the presence of sensor biases and missed detections. The robust track-to-track association is turned into the non-rigid point matching problem. The t-distribution mixture model is established to determine the correspondence between local tracks from different sensors. Moreover, to prevent unpaired tracks which are spatially close from matching wrongly, the Tikhonov regular term is imposed on the algorithm. Simulation results verify the effectiveness of the proposed algorithm compared with other competing algorithm. In a word, the proposed algorithm provides a reliable method to solved track-to-track association.

References

[1] Y. Bar-Shalom, H. Chen, Multisensor track-to-track association for tracks with dependent errors, J. Adv. Inf. Fusion 1 (1) (2006) 3–14

[2] H. Zhu, H. Leung, and K V. Yuen. A joint data association, registration, and fusion approach for distributed tracking[J]. Information Sciences An International Journal, 2015, 324(C): 186-196.

[3] Y. He, Q. Song, W. Xiong. A track registration-correlation algorithm based on fourier transform[J]. Acta Aeronautica ET Astronautica Sinica, 2010, 31(2): 356-362.

[4] D. Hambrick and W. D. Blair. Multisensor track association in the presence of bias[C]. IEEE Aerospace Conference, Washington, D.C., USA, 2014: 1-6.

[5] H.Y. Zhu and S.Y Han. Track-to-track association based on structural similarity in the presence of sensor biases[J]. Journal of Applied Mathematics, 2014, 1:1-8.

[6] H.Y. Zhu and C. Wang. Joint track-to-track association and sensor registration at the track level[J]. Digital Signal Processing, 2015, 41: 48-59.

[7] W. Tian, Y. Wang, and X.M. Shan, et al. Track-to-track association for biased data based on the reference topology feature[J]. IEEE Signal Processing Letters, 2014, 21(4): 449-453.

[8] K. Dong，H.P. Wang，Y. Liu. Anti-bias track association algorithm based on topology statistical distance[J]. Journal of Electronics &Information Technology, 2015, 37(1): 50-55.

[9] D. Huang, H. Leung, and E Bosse. A pseudo-measurement approach to simultaneous registration and track fusion[J]. IEEE Transactions on Aerospace & Electronic Systems, 2012, 48(3): 2315-2331.

[10] H.Y. Zhu and S. Chen. Track fusion in the presence of sensor biases[J]. IET Signal Processing, 2014, 8(9): 958-967.

[11] L. Qi Anti-bias track-to-track association algorithm based on distance detection[J]. Iet Radar Sonar Navigation, 2016.

[12] H.Y. Zhu, W. Wang, and C. Wang. Robust track-to-track association in the presence of sensor biases and missed detections[J]. Information Fusion, 2016, 27: 33-40.

[13] H.Y. Zhu, Y. Zhang, C. Wang. Anti-biases track-to-track association based on relaxation labeling[J]. Control & Decision, 2015, 30(4): 593-598.

[14] R. Hartley and A. Zisserman. Multiple View Geometry in Computer Vision[M]. Second Edition, Cambridge: UK, Cambridge University Press, 2004: 39-40

[15] S. X. Lee and G. J. Mclachlan. Finite mixtures of canonical fundamental skew t-distributions[J]. Statistics & Computing, 2016, 26(3): 573-589.

[16] D. Peel and G. J. Mclachlan. Robust mixture modelling using the t distribution[J]. Statistics & Computing, 2000, 10(4): 339-348.

[17] C.F.J Wu. On the convergence properties of the EM algorithm[J]. The Annals of statistics, 1983, 11(1): 95-103.

[18] C. Liu and D. B. Rubin. ML estimation of the t distribution using EM and its extensions, ECM and ECME[J]. Statistica Sinica, 1995, 5: 19-39.

[19] A. Myronenko and X. SONG. Point set registration: Coherent point drift[J]. IEEE Transactions on Software Engineering, 2010, 32(12): 2262-2275.